Crossover Interference in the Mouse

Karl W. Broman,*[,1] Lucy B. Rowe,[†] Gary A. Churchill[†] and Ken Paigen[†]

**Department of Biostatistics, Johns Hopkins University, Baltimore, Maryland 21205 and [†]The Jackson Laboratory, Bar Harbor, Maine 04609*

Manuscript received November 11, 2001
Accepted for publication January 3, 2002

ABSTRACT

We present an analysis of crossover interference in the mouse genome, on the basis of high-density genotype data from two reciprocal interspecific backcrosses, comprising 188 meioses. Overwhelming evidence was found for strong positive crossover interference with average strength greater than that implied by the Carter-Falconer map function. There was some evidence for interchromosomal variation in the level of interference, with smaller chromosomes exhibiting stronger interference. We further compared the observed numbers of crossovers to previous cytological observations on the numbers of chiasmata and evaluated evidence for the obligate chiasma hypothesis.

CROSSOVER interference may be defined as the nonrandom placement of crossovers, relative to one another, along chromosomes in meiosis. Interference was identified soon after the development of the first working models for the recombination process (Sturtevant 1915; Muller 1916). Strong evidence for positive crossover interference (with crossovers more evenly spaced than would be expected under random placement—historically observed as a lower frequency of double recombinants in adjacent intervals than would be expected under independence) has been obtained in many species (Zhao *et al.* 1995b). Investigations of interference have generally involved observed frequencies of rare multiple recombination events in sets of adjacent intervals (Zhao *et al.* 1995b). Such an approach requires many thousands of meioses, each informative for the same set of markers. Weinstein (1936), for example, studied seven loci in 28,239 *Drosophila melanogaster* offspring. Broman and Weber (2000), in a study of human crossover interference, considered the estimated locations of crossovers, on the basis of high-density genotype data, in a relatively small number of meioses; we make use of their approach to examine crossover interference in the mouse.

Meiotic recombination occurs after the chromosomes have duplicated. Homologous chromosome pairs line up together, forming tight bundles of four chromatids. Nonsister chromatids then synapse and exchange material; the locations at which this occurs are called chiasmata. The chiasmata are observed as crossovers in two of the four products of meiosis. (For a review of meiosis and the mechanism of recombination, see Roeder 1997.)

Interference is generally split into two aspects: chromatid interference and crossover interference. Chromatid interference is a dependence in the choice of strands involved in adjacent chiasmata. There is little consistent evidence for the presence of chromatid interference in experimental organisms (Zhao *et al.* 1995a), and inference about chromatid interference generally requires data on all four products of meiosis (tetrad data), which are not available in mammals. Thus we assume no chromatid interference throughout this work. Crossover interference (also known as chiasma interference) is defined as the nonrandom placement of chiasmata on individual chromatids. Under positive crossover interference, chiasmata are more evenly spaced, while under negative crossover interference, they are more clustered. Meiosis generally shows positive crossover interference (Zhao *et al.* 1995b), although exceptions do exist (Munz 1994). Interference is also under genetic control (Sym and Roeder 1994).

Positive interference (subsequently referred to as "interference" in this article) is important in meiosis in that, if there is a limited number of chiasmata per meiosis genome wide, interference will result in the chiasmata being more evenly distributed across chromosomes. Thus interference may constitute a biological mechanism to ensure that the smallest chromosomes will have at least one chiasma, which is necessary for the proper segregation of chromosomes (reviewed in Egel 1995; Roeder 1997). Yeast mutants for which interference is absent show a greater rate of nondisjunction (Sym and Roeder 1994; Chua and Roeder 1997).

In addition to its biological role in chromosome disjunction, crossover interference has made possible more accurate genetic analysis by enabling the detection of technical errors in dense maps. In the construction of the data sets used for the analysis described herein, all cases of single-locus double crossovers that were rigorously retyped proved to be technical artifacts rather than closely spaced crossover events. Thus the phenomenon of interference facilitates genetic map construction and the detection of genotyping errors.

Good evidence exists for positive interference in mice,

[1]*Corresponding author:* Department of Biostatistics, Johns Hopkins University, 615 N. Wolfe St., Baltimore, MD 21205.
E-mail: kbroman@jhsph.edu

though a detailed characterization has not yet been achieved. Cytogenetic evidence for interference has been obtained by Hultén and colleagues (Hultén *et al.* 1995; Lawrie *et al.* 1995) through analysis of chiasma locations in oocytes and spermatocytes. Several groups (Blank *et al.* 1988; Ceci *et al.* 1989; Kingsley *et al.* 1989) have shown that the distribution of the number of crossovers per chromosome differs significantly from that expected under the assumption of no interference. Weeks *et al.* (1994) fit several mathematical models for interference to multilocus genotype data on mouse chromosomes 1 and 12 and found significant evidence for positive interference.

Numerous mathematical models for recombination, incorporating interference, have been developed. (For reviews, see Karlin and Liberman 1994 and McPeek and Speed 1995.) We focus on the gamma model, as it has been shown to provide a reasonable fit to recombination data from numerous organisms (McPeek and Speed 1995; Broman and Weber 2000). In the gamma model, the locations of the chiasmata on the four-strand bundle are determined according to a stationary renewal process with increments being gamma distributed with shape and rate parameters ν and 2ν, respectively, for $\nu > 0$. In other words, the distances between chiasmata are independent and follow a gamma distribution having mean 1/2 and standard deviation (SD) $1/(2\sqrt{\nu})$ M. (For a detailed discussion of renewal processes, see Cox 1962.) Under the assumption of no chromatid interference, the locations of crossovers on a random meiotic product are obtained by "thinning" the chiasma process: Chiasmata on the four-strand bundle are retained as crossovers independently with probability 1/2 (since each chiasma involves two of the four chromatids). The shape and rate parameters of the gamma model satisfy the constraint that the average interchiasma distance is 0.5 M, and so the average intercrossover distance is 1 M. The parameter ν is a unitless measure of the strength of interference: The case $\nu = 1$ corresponds to no interference; $\nu > 1$ (<1) corresponds to positive (negative) crossover interference. These models have a long history (see McPeek and Speed 1995), having first been proposed by Fisher *et al.* (1947). Foss *et al.* (1993) and Foss and Stahl (1995) revived interest in these models after describing a mechanism for recombination that gives rise to such models. In their biological model, chiasmata must be separated by a fixed number, m, of intermediate gene conversion events. If the locations of the chiasmata and intermediate events are at random (*i.e.*, according to a Poisson process), the locations of the chiasmata are according to the χ^2 model, which is a special case of the gamma model with $\nu = m + 1$ for a nonnegative integer m, so called because the gamma distribution with shape and rate parameters $m + 1$ and $2(m + 1)$, respectively, is a scaled version of a χ^2 distribution with $2(m + 1)$ d.f. The χ^2 model was also considered by Zhao *et al.* (1995b) and Lin and Speed (1996).

Rowe *et al.* (1994) established two interspecific backcross DNA panels as a community resource for genetic mapping. The two backcrosses, (C57BL/6J × *Mus spretus*)F_1 × C57BL/6J and (C57BL/6J × SPRET/Ei)F_1 × SPRET/Ei, contain 94 N_2 animals each, have genetically identical F_1 parents, and have been genotyped at 1372 and 4913 genetic markers, respectively. The high-density genotype data allow a relatively precise localization of all recombination events in the corresponding meioses, which may then be used to estimate, for each chromosome, the distribution of the number of chiasmata per meiosis and the level of crossover interference. The results of this study provide strong, genome-wide evidence for positive crossover interference in the mouse, with average strength somewhat greater than that implied by the Carter-Falconer map function (Carter and Falconer 1951). In addition, we observed some evidence for interchromosomal variation in the level of interference.

MATERIALS AND METHODS

Mapping panels and genotype data: Rowe *et al.* (1994) described the establishment of two interspecific backcross DNA panels, (C57BL/6J × *M. spretus*)F_1 × C57BL/6J and (C57BL/6J × SPRET/Ei)F_1 × SPRET/Ei, denoted BSB and BSS, respectively. These crosses are composed of 94 N_2 individuals each, which at the time of this analysis (September 2000) had been genotyped for 1372 and 4913 genetic markers, respectively, with 904 of the markers typed in common between the two crosses. (The current genotype data are publicly available: http://www.jax.org/resources/documents/cmdata/ftp.html.)

The *M. spretus* strain was derived from the same breeding colony as the SPRET/Ei strain, but separated after 18 generations of inbreeding (21 total generations of inbreeding for the *M. spretus* parents and 28 generations of inbreeding for the SPRET/Ei parents used in these experiments). Thus the F_1 parents in the two crosses may be treated as genetically identical. Indeed, the estimated genetic maps for the two crosses were not significantly different, and so the combined 188 meioses were considered together. We formed an integrated genetic map, taking the 904 common markers as a framework, using linear interpolation between the two maps to establish marker order, and reestimating the genetic distances between markers by the Lander-Green algorithm (Lander and Green 1987). The average distances between markers were 1.0, 0.28, and 0.26 cM in BSB, BSS, and overall, respectively.

The data originate from multiple laboratories worldwide, using a common set of backcross DNAs to map DNA-based markers of interest, and are curated at The Jackson Laboratory. Since all the markers were mapped on the same set of DNAs, marker order was determined from the data with little ambiguity. Where possible, when new single-locus double crossovers were observed, these were repeated by the investigator for confirmation. In all cases of rigorous retesting, these single-locus double crossovers were shown to be due to laboratory error. On the basis of this observation, we have made the assumption that all untested single-locus double crossovers are also due to laboratory error, and we have omitted them from the data prior to analysis.

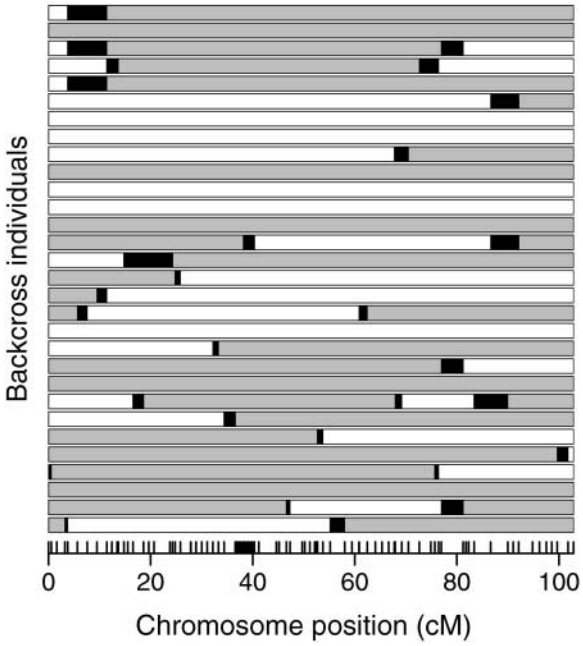

FIGURE 1.—Parental origin of DNA in the recombinant chromosome 1 in the first 15 individuals from each of the two backcrosses. Open segments denote C57BL/6J DNA; shaded segments denote SPRET/Ei or *M. spretus* DNA. The smaller solid segments are the noninformative segments in which a recombination occurred. The ticks at the bottom indicate the locations of the genetic markers.

The locations of all recombination events on all chromosomes in each of the 188 meioses were identified. Although, in reality, each crossover can be localized only to a position within the interval between the typed markers flanking the recombination event, the intervals into which the crossovers could be placed were generally quite small. For example, Figure 1 shows the parental origin of DNA for 30 of the chromosome 1's (the first 15 mice from each cross). The solid bars, which represent the extent to which we can localize crossovers, are quite small, especially in comparison to the distances between crossovers. (The medians of the lengths of the intervals to which crossovers could be localized were 3.0 and 1.6 cM for the BSB and BSS crosses, respectively; the maximum lengths were 17.0 and 8.1 cM, respectively.) Each crossover was assumed to have occurred at the midpoint of the interval between its two flanking typed markers, and the small error introduced by this convention was ignored. We further assumed that all crossovers were observed (*i.e.*, that no double crossovers between typed markers occurred).

Estimation of chromosome lengths: Estimation of the genetic lengths of chromosomes is described above. Standard errors (SEs) of these lengths were estimated by calculating the SE of the average number of recombination events observed for each chromosome. The SEs of chromosome lengths ranged from 3.7 to 5.5 cM.

The genetic lengths derived from the BSB/BSS data were compared to estimates based on counts of chiasmata in C3H/HeH×101/H oocytes by cytological investigation; numbers of chiasmata were determined for each autosome in 58 oocytes (LAWRIE *et al.* 1995) and for the X chromosome in 57 oocytes (HULTÉN *et al.* 1995). SEs of the chiasma-based estimates of genetic lengths were derived from the reported SDs of the numbers of chiasmata.

Both sets of estimated genetic lengths were compared to the physical lengths reported in EVANS (1996). The physical lengths, originally reported as percentages, were scaled to megabase lengths with the assumption of a total genome length of 3000 Mb.

Estimation of the distribution of the number of chiasmata: Data on the observed numbers of crossovers for each chromosome allow estimation of the underlying distribution of the number of chiasmata per meiotic product. Let n denote the number of chiasmata on the four-strand bundle, and let m denote the number of crossovers on a random meiotic product. We assume that n follows some distribution $\boldsymbol{p} = (p_0, p_1, p_2, \ldots)$. Under no chromatid interference, m, given n, is distributed as binomial $(n, \frac{1}{2})$. The distribution of the number of chiasmata, $\boldsymbol{p}$, may be estimated by a version of the expectation-maximization (EM) algorithm (DEMPSTER *et al.* 1977), as described by OTT (1996); see also YU and FEINGOLD (2001). This was performed separately for an unrestricted distribution and under the constraint $p_0 = 0$ (the obligate chiasma hypothesis).

SEs for the frequencies of chiasmata were estimated by a parametric bootstrap: Counts of crossovers for 188 meioses were simulated using the estimated distribution of the number of chiasmata, with the assumption of no chromatid interference. These counts were used to reestimate the chiasma frequencies. We performed 250 bootstrap replicates and estimated the SEs of the chiasma frequencies by the SDs of the estimates across bootstrap replicates.

Fit of the gamma model: The gamma model provides a measure of the strength of interference through the parameter ν. The gamma model was fit by the method of BROMAN and WEBER (2000), which we briefly describe. For data on crossover locations on a set of independent meiotic products, the gamma model provides a likelihood function of a single parameter, ν. The maximum-likelihood estimate (MLE) of ν was obtained by numerical optimization of this likelihood. Approximate confidence intervals were obtained as likelihood support intervals: the intervals for which the likelihood for ν was within a factor of 10 of its maximum. A likelihood-ratio (LR) test was used to assess the significance of variation between the chromosome-specific estimates of ν.

The quality of the fit of the gamma model was assessed by comparing the observed distances between crossovers, on meiotic products exhibiting exactly two crossovers, to that expected under the gamma model, with the chromosome-specific estimates of the parameter ν. The fitted distributions were calculated by numerical integration.

RESULTS

Crossover and chiasma distributions: The distributions of the numbers of crossovers per chromosome are displayed in Table 1. The sum of each row in this table is 188, the total number of meioses in the two backcross panels. Four meiotic products exhibited three crossovers. Chromosome 19 showed no double crossovers.

The data in Table 1 were used to estimate, under the assumption of no chromatid interference, the underlying distribution of the number of chiasmata per four-strand bundle (the distribution $\boldsymbol{p}$ in MATERIALS AND METHODS) for each chromosome. These estimated distributions (as percentages) are displayed in Table 2. (Note that the estimated SEs of the frequencies were generally in the range 5–10%.) Chromosomes 1 and 19 are particularly interesting. For chromosome 1, it was

TABLE 1

Observed distributions of the number of crossovers per meiotic product

Chromosome	No. crossovers			
	0	1	2	3
1	53	87	46	2
2	59	95	33	1
3	71	92	25	0
4	55	99	33	1
5	58	105	25	0
6	86	78	24	0
7	73	95	20	0
8	78	93	17	0
9	79	91	18	0
10	78	103	7	0
11	80	88	20	0
12	90	90	8	0
13	72	108	8	0
14	76	108	4	0
15	88	98	2	0
16	80	101	7	0
17	96	91	1	0
18	112	74	2	0
19	91	97	0	0
X	67	98	23	0

TABLE 2

Estimated distributions (as percentages) of the number of chiasmata per meiosis under the assumption of no chromatid interference

Chromosome	No. chiasmata				Obligate chiasma $\log_2$ LR
	0	1	2	3	
1	5	1	85	9	0.38
2	0	30	66	4	0.00
3	2	45	53	0	0.06
4	0	25	75	0	0.00
5	0	40	60	0	0.00
6	17	34	49	0	3.72
7	0	57	43	0	0.00
8	1	63	36	0	0.02
9	3	59	38	0	0.14
10	0	84	17	0	0.00
11	6	51	43	0	0.55
12	4	79	17	0	0.25
13	0	80	20	0	0.00
14	0	90	10	0	0.00
15	0	96	4	0	0.00
16	0	84	16	0	0.00
17	3	95	2	0	0.10
18	21	75	4	0	6.19
19	0	100	0	0	0.00
X	0	49	51	0	0.00

Estimated standard errors for these values are in the range 5–10%. The last column gives the $\log_2$ LR testing the hypothesis of an obligate chiasma. The values in some rows do not sum to 100, due to round-off error.

estimated that the majority of meioses have exactly two chiasmata, while chromosome 19 appears to exhibit exactly one chiasma per meiosis. It should be noted that these estimated distributions suffer from considerable imprecision. For example, the 95% confidence interval for the probability of exactly two chiasmata on chromosome 1 ranges from 58 to 99%.

The estimation procedure allowed us to examine the hypothesis of an obligate chiasma on each four-strand bundle. For most chromosomes, the probability of no chiasma was estimated to be 0. The last column in Table 2 contains the log (base 2) likelihood ratio for testing the null hypothesis of an obligate chiasma. Large values of the $\log_2$ LR indicate evidence *against* an obligate chiasma. Only chromosomes 6 and 18 show any departure from an obligate chiasma. These chromosomes exhibited a large number of meiotic products with no crossovers (see Table 1). However, the evidence against the obligate chiasma hypothesis is not strong. If consideration is made of the 20 statistical tests performed, the result for chromosome 18 is only marginally statistically significant.

In Figure 2A, the estimated genetic lengths of the chromosomes are shown, as derived from the BSB/BSS data and through cytological inspection of the number of chiasmata in oocytes (Hultén *et al.* 1995; Lawrie *et al.* 1995). The lengths correspond reasonably well, though the BSB/BSS data gave longer chromosomal lengths for 17 of the 20 chromosomes. The differences in the estimated lengths were greatest for the smaller chromosomes. Note that for chromosome 18, the estimated genetic length derived from the BSB/BSS data was quite small relative to that reported by Lawrie *et al.* (1995). The total genetic length of the mouse genome was estimated to be 13.9 M (an average of 27.8 chiasmata per meiosis) on the basis of the BSB/BSS data and 12.6 M (an average of 25.3 chiasmata per meiosis) on the basis of the chiasma counts.

In Figure 2B, these lengths are plotted against the estimated physical lengths reported by Evans (1996). The data from Lawrie *et al.* (1995) showed a biphasic relationship between genetic and physical lengths, with chromosomes <150 Mb having a nearly constant length of 50 cM (one chiasma per meiosis), while for longer chromosomes, the genetic lengths increase approximately linearly with physical length. For the lengths derived from the BSB/BSS data (the circles in Figure 2), the biphasic relationship is less clear, although this may be a result of the imprecision in the estimates.

It is interesting to note that the SEs of the estimated genetic lengths derived with the BSB/BSS data are considerably larger than those based on chiasma counts, in spite of the fact that the BSB/BSS data comprise 188 meioses, while only 57 (X chromosome) or 58 (autosomes) oocytes were used for the counts of chiasmata (Hultén *et al.* 1995; Lawrie *et al.* 1995). This is a result

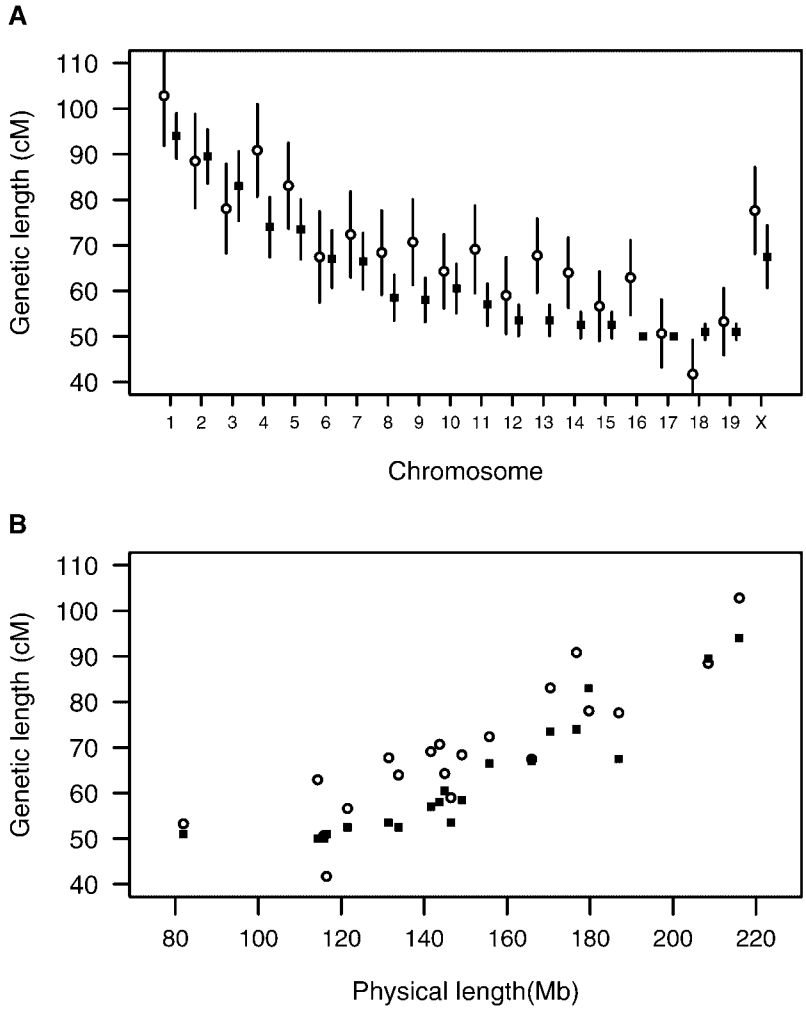

FIGURE 2.—(A) Estimated genetic lengths, with approximate confidence intervals, for each chromosome for the BSB/BSS data (○) and as reported in HULTÉN *et al.* (1995) and LAWRIE *et al.* (1995), on the basis of counts of chiasmata (■). (B) Genetic length *vs.* physical length for each chromosome.

of the fact that crossover counts are inherently more variable than chiasma counts because of the sampling of chromatids (each chiasma involves two of the four possible strands). Let n denote the number of chiasmata for a chromosome, and let m denote the number of crossovers on that chromosome in a random meiotic product. Then, under no chromatid interference,

$$\begin{aligned}\text{var}(m) &= E[\text{var}(m|n)] + \text{var}[E(m|n)] \\ &= E(n/4) + \text{var}(n/2) \\ &= [2L + \text{var}(n)]/4,\end{aligned}$$

where $L = E(n)/2$ is the genetic length of the chromosome (in morgans). This is dominated by the genetic length, L, since $\text{var}(n) < 0.1$ (see LAWRIE *et al.* 1995), while $2L$ is in the range 1–2. Counts of crossovers thus provide less precise estimates of the genetic lengths of chromosomes. On the other hand, recombinational information may provide more precise estimates of the locations of crossovers, which are of principal interest in an analysis of interference.

Figure 3 provides a detailed view of the crossover process in the mouse genome; this figure was inspired by Figure 4 in LAWRIE *et al.* (1995). The circles and the tick marks below and to the left indicate the locations of the pair of crossovers on meiotic products with exactly two crossovers. Circles above the dotted diagonal line correspond to crossovers separated by <20 cM. Ten out of the 323 pairs of crossovers were separated by <20 cM. The presence of so few points above this line indicates strong positive crossover interference in the mouse. If there were no crossover interference, the points would be uniformly distributed over the triangle defined by the solid diagonal line, and so we would expect 145 out of the 323 pairs of crossovers to be separated by <20 cM. Note that the ticks on the right indicate the locations of markers on the genetic map; the maps are quite dense, though there remain a number of gaps. The ticks at the top indicate the locations of crossovers on meiotic products with exactly one crossover; these are approximately evenly distributed. The x's indicate the locations of crossovers on the four triple-crossover meiotic products. Note that these crossovers are widely spaced, with the closest pair of crossovers separated by ~18 cM.

Levels of interference: Figure 4 displays the chromosome-specific estimates of the interference parameter ν,

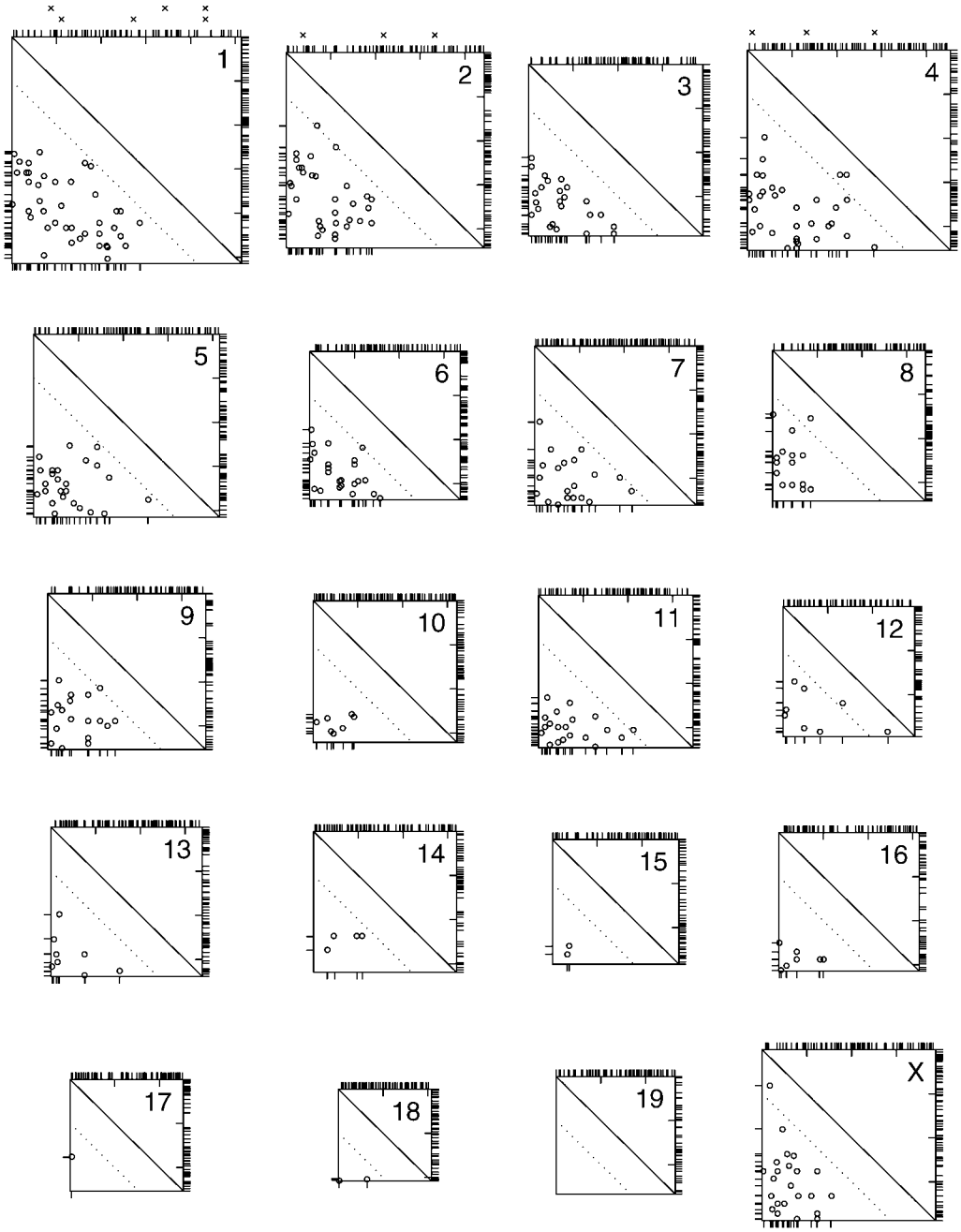

FIGURE 3.—Crossover locations for all chromosomes. Each square represents a chromosome, with the centromere at the top and left and the telomere at the bottom and right. Ticks on the right indicate the locations of the genetic markers. The circles indicate the locations of the pair of crossovers on meiotic products exhibiting exactly two crossovers, with the location of the proximal and distal crossovers shown below and to the left, respectively. Circles above the dotted diagnonal line are crossovers separated by <20 cM. The locations of crossovers on meiotic products that exhibit exactly one crossover are shown at the top. The x's above chromosomes 1, 2, and 4 indicate the locations of crossovers on triple-crossover meiotic products.

for the gamma model, with likelihood support intervals (the values of ν for which the likelihood was within a factor of 10 of its maximum) indicating plausible values of ν. A horizontal line is plotted at $\hat{\nu} = 11.3$ (SE $\approx$ 0.7), the estimate obtained after pooling data across chromosomes. Note that for chromosome 19, none of the 188 meiotic products exhibited more than one crossover, and so $\hat{\nu} = \infty$; the lower bound of the likelihood support interval was 35. These data show clear evidence for interference on all chromosomes. The no interference model corresponds to the value $\nu = 1$; the likelihood support intervals for ν for all chromosomes are well above the value 1.

Chromosomes 4 and 12 exhibit a lower level of interference than the other chromosomes. These were the only chromosomes exhibiting more than one pair of crossovers separated by <20 cM (see Figure 3). A pair of crossovers on chromosome 12 were separated by only 10 cM.

A likelihood-ratio test to assess interchromosomal variation in the level of interference indicated strong evidence for such variation ($P \approx 10^{-5}$). Figure 5 displays the estimates of ν as a function of chromosome length. Smaller chromosomes are seen to generally exhibit stronger levels of interference, although the confidence intervals for the chromosome lengths and levels of interference are wide, indicating considerable uncertainty in each.

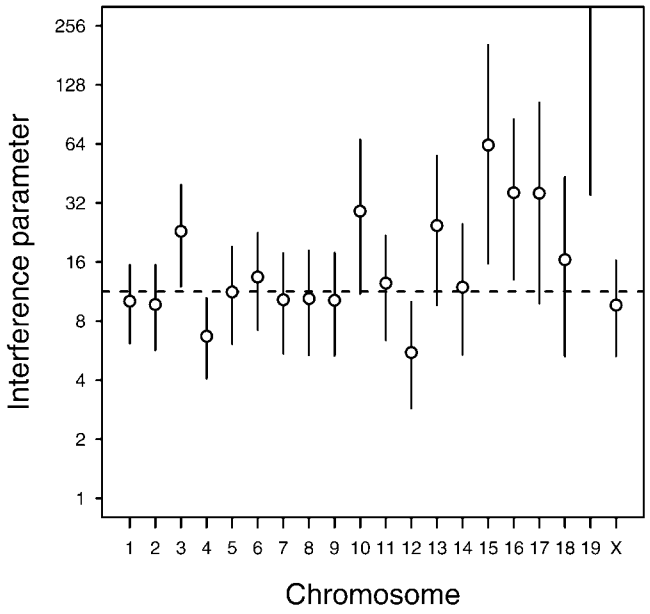

FIGURE 4.—Estimates of the interference parameter ν from the gamma model for each chromosome, with approximate confidence intervals. A horizontal line is plotted at the pooled estimate of ν. Note that chromosome 19 gave $\hat{\nu} = \infty$.

Figure 6 displays, for chromosomes 1–4, the distribution of the distance between crossovers on meiotic products exhibiting exactly two crossovers. The solid curves correspond to the fitted distributions for the gamma model. The dashed curves correspond to the fitted distributions in the case of no crossover interference. The dearth of closely spaced crossovers (also seen in Figure 3) indicates strong evidence for positive crossover interference. The gamma model provides a reasonably good fit to these data. While the fit is not perfect, this is in part the result of a paucity of data. For example, chromosome 1 showed 46 meiotic products with exactly two crossovers; the histogram at the top left of Figure 6 does not deviate significantly from the fitted curve under the gamma model.

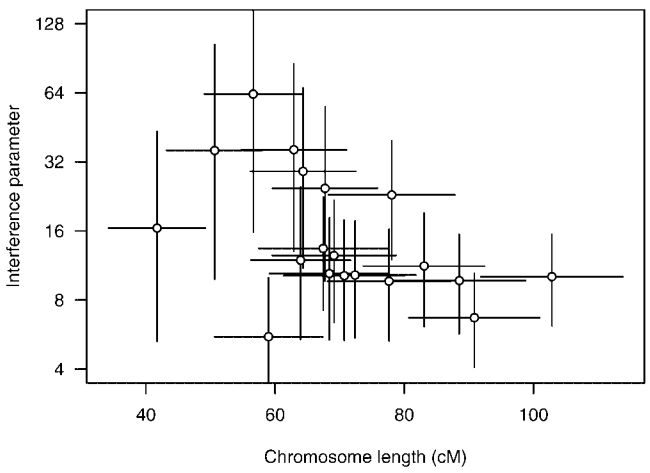

FIGURE 5.—Estimates of the interference parameter ν from the gamma model, plotted against chromosome length. Vertical and horizontal segments indicate approximate confidence intervals.

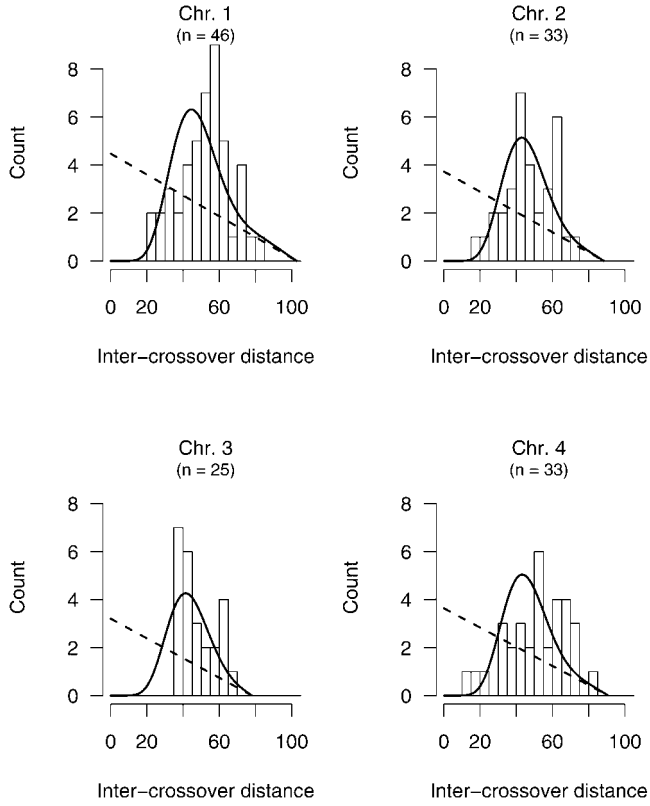

FIGURE 6.—Observed distributions of the distance between crossovers for meiotic products exhibiting exactly two crossovers. (n indicates the number of such products.) The solid and dashed curves correspond to the fitted distributions under the gamma and no interference models, respectively.

DISCUSSION

The results of this study provide strong genome-wide evidence for positive crossover interference in the mouse. A gamma model with $\nu = 7.6$ has a map function that corresponds approximately to the Carter-Falconer map function (ZHAO and SPEED 1996). The pooled estimate of ν for these data was 11.3, indicating that the average strength of crossover interference in the mouse may be stronger than that implied by the Carter-Falconer map function. Note, for comparison, that $\nu = 1$ under no interference, and $\hat{\nu} = 4.3$ is the estimated level of interference in humans (BROMAN and WEBER 2000). Crossover interference in the mouse appears to be extremely strong.

It is important to emphasize that we analyzed a pair of reciprocal interspecific backcrosses with a common female F_1 parent. Thus these conclusions may not exactly model either male meiosis or crosses using other mouse strain combinations.

Numerous approximations were made in this analysis.

We assumed that the markers were in the correct order and that the intermarker distances were known exactly. We assumed that all crossovers were observed and that the imprecision in the localization of crossovers was unimportant. Finally, we assumed that the level of interference was constant, relative to genetic distance, along each chromosome. (It will be valuable to revisit this work once the physical locations of markers become available, since interference may act on the physical scale. The inhomogeneity in recombination frequency along chromosomes will make such an investigation difficult, but also more interesting.)

In spite of these approximations, the estimated levels of interference are likely reasonable, though their estimated SEs are somewhat too small. For example, chromosome 12 showed a lower level of interference than any other chromosome ($\hat{\nu} = 5.5$), largely the result of two tight double crossovers, including a pair of crossovers separated by only 10 cM (see Figure 3). If the estimated genetic distance between these crossovers had been larger, the estimated level of interference on chromosome 12 would be stronger. Estimates of the interference parameter are clearly sensitive to the distance between tightly spaced double crossovers.

Our results rely, in part, on the appropriateness of the gamma model. While the gamma model provides a reasonable fit to these data (see Figure 6), it fails to capture all of the biological details of the recombination process. For example, it does not require the presence of at least one chiasma on the four-strand bundle. The gamma model should be viewed as a device for estimating the strength of crossover interference. While more elaborate mathematical models might conform better to what is known about the biological mechanism of the recombination process, the data are not sufficient to discriminate between such models, and the estimated levels of interference would likely be little changed.

We observed some evidence for variation in interference between chromosomes, with smaller chromosomes showing a greater level of interference (see Figure 5). This is in contradiction to previous results on the relationship between chromosome size and the strength of interference; Kaback *et al.* (1999) reported that, in yeast, smaller chromosomes exhibit a *lower* level of interference. The imprecision in the estimates of both the levels of interference and the genetic lengths of the chromosomes makes the assessment of this relationship difficult.

Further, the estimates of the levels of interference for small chromosomes appear to be subject to a positive bias (*i.e.*, the observed estimates are likely too large). We conducted a small computer simulation study (data not shown) to investigate the possibility of bias for different levels of interference and different chromosome lengths. For chromosomes <60 cM, the bias is $\sim$0.1–0.3 on the $\log_2$ scale; for large chromosomes, the bias was negligible. (It should be noted that, because the MLE of the interference parameter ν is infinite when no meiotic products exhibit more than one crossover, the bias of the MLE is also infinite, unless one conditions on the presence of at least one meiotic product with more than one crossover.) However, it does not appear that this bias is sufficient to explain the relationship between chromosome size and level of interference observed in these data.

The observed numbers of crossovers per chromosome allowed us to investigate the hypothesis of an obligate chiasma per four-strand bundle. Only two chromosomes (6 and 18) provided any evidence against an obligate chiasma, and this evidence was weak. We conclude that these data are consistent with the obligate chiasma hypothesis.

It is interesting to note the apparent relationship between frequency of recombination and degree of interference: the mouse and human genomes are similar in size, but the human has a higher crossover frequency and a lower level of interference (Broman and Weber 2000). The human genome has been estimated to be $\sim$44 M (female) or 27 M (male), or an average of 35.8 M (Broman *et al.* 1998). The mouse genome size estimated from these interspecific backcross data is 13.9 M. (The degree of difference between sex-specific recombination frequencies varies among mouse strains, but is much lower than in humans.) Remarkably, the ratio of the estimated genetic lengths of the human and mouse genomes (35.8 M human/13.9 M mouse = 2.6) is the reciprocal of the ratio of the estimated interference parameters, ν (11.3 mouse/4.3 human = 2.6). (This observation should be considered with great care, as the interference parameter is measured on an arbitrary scale.) However, Broman and Weber (2000) found no significant difference in the degree of interference between the sexes in humans, while there is a 1.6-fold difference in the frequency of recombination. This suggests that the control of interference may be species specific, with additional sex-specific control of recombination in some animals.

The mouse backcross data used here give an estimate of an average chiasma frequency of 27.8 per genome. This agrees well with frequencies observed by others on the basis of direct cytological observations: 25.3 average chiasmata per cell reported by Hultén and colleagues (Hultén *et al.* 1995; Lawrie *et al.* 1995) and 27.5 chiasmata per cell observed by Polani (1972). The discrepancy between the estimated genetic lengths based on BSB/BSS data and those reported by Lawrie *et al.* (1995) was greatest for the small chromosomes. Note that the greater level of recombination in these data is the opposite of what one would expect in a cross between such divergent strains. With 20 centromeres, 28 chiasmata approaches the minimum necessary to ensure proper disjunction at meiosis. Thus it can be predicted that the mouse may have one of the highest levels of crossover interference, while organisms with very high

ratios of recombination frequency to centromere count have very low or no interference (see Sym and Roeder 1994).

Recently, synaptonemal complex proteins have been implicated in the control of crossover interference. In both yeast and tomato, interference has been shown to be limited to portions of chromosomes involved in synaptonemal complexes (Chua and Roeder 1997). In yeast, null mutations in the synaptonemal complex proteins tam1 and zip1 show no reduction in recombination frequency but a marked reduction in interference (Sym and Roeder 1994; Chua and Roeder 1997). The results of our study suggest that a comparison of mouse and human synaptonemal complex proteins may reveal insights into the mechanism of modulation of interference.

The backcross panels established by Rowe *et al.* (1994) are a valuable resource, both for the high-density genetic maps of the mouse genome that they provide and for the analysis of crossover interference described herein. Our analysis relied on high-quality, high-density genotype data, which can be obtained only through careful curation, including the resolution of apparent genotyping errors. While data on substantially more meioses, combined with information on the physical locations of genetic markers, will provide a more detailed view of the recombination process, this study and these backcross panels have succeeded in providing the first complete characterization of crossover interference in the mouse.

Śaunak Sen provided valuable advice on Figure 3.

LITERATURE CITED

Blank, R. D., G. R. Campbell, A. Calabro and P. D'Eustachio, 1988 A linkage map of mouse chromosome 12: localization of Igh and effects of sex and interference on recombination. Genetics **120:** 1073–1083.

Broman, K. W., and J. L. Weber, 2000 Characterization of human crossover interference. Am. J. Hum. Genet. **66:** 1911–1926.

Broman, K. W., J. C. Murray, V. C. Sheffield, R. L. White and J. L. Weber, 1998 Comprehensive human genetic maps: individual and sex-specific variation in recombination. Am. J. Hum. Genet. **63:** 861–869.

Carter, T. C., and D. S. Falconer, 1951 Stocks for detecting linkage in the mouse, and the theory of their design. J. Genet. **50:** 307–323.

Ceci, J. D., L. D. Siracusa, N. A. Jenkins and N. G. Copeland, 1989 A molecular genetic linkage map of mouse chromosome 4 including the localization of several proto-oncogenes. Genomics **5:** 699–709.

Chua, P. R., and G. S. Roeder, 1997 Tam1, a telomere-associated meiotic protein, functions in chromosome synapsis and crossover interference. Genes Dev. **11:** 1786–1800.

Cox, D. R., 1962 *Renewal Theory.* Methuen, London.

Dempster, A., N. Laird and D. Rubin, 1977 Maximum likelihood from incomplete data via the EM algorithm. J. R. Stat. Soc. Ser. B **39:** 1–22.

Egel, R., 1995 The synaptonemal complex and the distribution of meiotic recombination events. Trends Genet. **11:** 206–208.

Evans, E. P., 1996 Standard idiogram, p. 1446 in *Genetic Variants and Strains of the Laboratory Mouse*, Vol. 2, Ed. 3, edited by M. F. Lyon, S. Rastan and S. D. M. Brown. Oxford University Press, London.

Fisher, R. A., M. F. Lyon and A. R. G. Owen, 1947 The sex chromosomes in the house mouse. Heredity **1:** 335–365.

Foss, E. J., and F. W. Stahl, 1995 A test of a counting model for chiasma interference. Genetics **139:** 1201–1209.

Foss, E. J., R. Lande, F. W. Stahl and C. M. Steinberg, 1993 Chiasma interference as a function of genetic distance. Genetics **133:** 681–691.

Hultén, M. A., C. Tease and N. M. Lawrie, 1995 Chiasma-based genetic map of the mouse X chromosome. Chromosoma **104:** 223–227.

Kaback, D. B., D. Barber, J. Mahon, J. Lamb and J. You, 1999 Chromosome size-dependent control of meiotic reciprocal recombination in *Saccharomyces cerevisiae*: the role of crossover interference. Genetics **152:** 1475–1486.

Karlin, S., and U. Liberman, 1994 Theoretical recombination processes incorporating interference effects. Theor. Popul. Biol. **46:** 198–231.

Kingsley, D. M., N. A. Jenkins and N. G. Copeland, 1989 A molecular genetic linkage map of mouse chromosome 9 with regional localizations for the Gsta, T3g, Ets-1 and Ldlr loci. Genetics **123:** 165–172.

Lander, E. S., and P. Green, 1987 Construction of multilocus genetic linkage maps in humans. Proc. Natl. Acad. Sci. USA **84:** 2363–2367.

Lawrie, N. M., C. Tease and M. A. Hultén, 1995 Chiasma frequency, distribution and interference maps of mouse autosomes. Chromosoma **104:** 308–314.

Lin, S., and T. P. Speed, 1996 Incorporating crossover interference into pedigree analysis using the χ^2 model. Hum. Hered. **46:** 315–322.

McPeek, M. S., and T. P. Speed, 1995 Modeling interference in genetic recombination. Genetics **139:** 1031–1044.

Muller, H. J., 1916 The mechanism of crossing-over. Am. Nat. **50:** 193–221, 284–305, 350–366, 421–434.

Munz, P., 1994 An analysis of interference in the fission yeast *Schizosaccharomyces pombe*. Genetics **137:** 701–707.

Ott, J., 1996 Estimating crossover frequencies and testing for numerical interference with highly polymorphic markers, pp. 49–63 in *Genetic Mapping and DNA Sequencing*: *IMA Volumes in Mathematics and Its Applications*, Vol. 81, edited by T. Speed and M. S. Waterman. Springer-Verlag, New York.

Polani, P. E., 1972 Centromere localization at meiosis and the position of chiasmata in the male and female mouse. Chromosoma **36:** 343–374.

Roeder, G. S., 1997 Meiotic chromosomes: it takes two to tango. Genes Dev. **11:** 2600–2621.

Rowe, L. B., J. H. Nadeau, R. Turner, W. N. Frankel, V. A. Letts *et al.*, 1994 Maps from two interspecific backcross DNA panels available as a community genetic mapping resource. Mamm. Genome **5:** 253–274.

Sturtevant, A. H., 1915 The behaviour of the chromosomes as studied through linkage. Z. Indukt. Abstammungs Vererbungsl. **13:** 234–297.

Sym, M., and G. S. Roeder, 1994 Crossover interference is abolished in the absence of a synaptonemal complex protein. Cell **79:** 283–292.

Weeks, D. E., J. Ott and G. M. Lathrop, 1994 Detection of genetic interference: simulation studies and mouse data. Genetics **136:** 1217–1226.

Weinstein, A., 1936 The theory of multiple-strand crossing over. Genetics **21:** 155–199.

Yu, K., and E. Feingold, 2001 Estimating the frequency distribution of crossovers during meiosis from recombination data. Biometrics **57:** 427–434.

Zhao, H., and T. P. Speed, 1996 On genetic map functions. Genetics **142:** 1369–1377.

Zhao, H., M. S. McPeek and T. P. Speed, 1995a Statistical analysis of chromatid interference. Genetics **139:** 1057–1065.

Zhao, H., T. P. Speed and M. S. McPeek, 1995b Statistical analysis of crossover interference using the chi-square model. Genetics **139:** 1045–1056.

Communicating editor: J. Rine